GA–A26402

# LOW-Z SHELL PELLET EXPERIMENTS ON DIII-D

by
E.M. HOLLMANN, A.N. JAMES, P.B. PARKS, T.E. EVANS,
D.A. HUMPHREYS, G.L. JACKSON, T.C. JERNIGAN, R.J. LA HAYE,
E.J. STRAIT, W.P. WEST, W. WU, and J.H. YU

MARCH 2009

GENERAL ATOMICS

## DISCLAIMER

GA–A26402

# LOW-Z SHELL PELLET EXPERIMENTS ON DIII-D

by
E.M. HOLLMANN,* A.N. JAMES, P.B. PARKS, T.E. EVANS,
D.A. HUMPHREYS, G.L. JACKSON, T.C. JERNIGAN,† R.J. LA HAYE,
E.J. STRAIT, W.P. WEST, W. WU, and J.H. YU*

This is a preprint of a paper to be presented at the 16th International Conf. on Atomic Processes in Plasmas, in Monterey, California, March 22–23, 2009 and to be published in the *Proceedings.*

*University of California-San Diego, La Jolla, California.
†Oak Ridge National Laboratory, Oak Ridge, Tennessee.

Work supported by
the U.S. Department of Energy
under DE-FG02-07ER54917, DE-FC02-04ER54698,
and DE-AC05-00OR22725

GENERAL ATOMICS PROJECT 30200
MARCH 2009

GENERAL ATOMICS

# ABSTRACT

Small (*o.d.* = 1.8 mm, $t$ = 0.37 mm) polystyrene shells filled with either pressurized argon gas or boron powder have been fired into DIII-D plasmas for disruption mitigation experiments. The pellet shells were observed to burn up at $\rho \approx 0.5$, roughly consistent with ablation rate calculations. Pellet slowing from 350 m/s down to 100 m/s was observed, which is not well-understood at present. Negligible plasma current contraction or MHD onset were seen as a result of the shell burn-up in the plasma edge, consistent with calculations. The pellet payloads were observed to ionize rapidly in the pellet vicinity (<1 cm radius) and rapid (<15 ms) mixing through the plasma core was observed.

# 1. INTRODUCTION

Developing a method for safely and rapidly shutting down tokamak discharges in the event of an unavoidable disruption is a high priority for the planned next generation tokamak ITER [1]. Presently, the rapid shutdown technique envisioned for ITER is massive gas injection (MGI) of inert gas such as Ne or Ar into the plasma edge. MGI is relatively straightforward to implement and works well for shutting down present-day tokamak discharges rapidly, with significantly reduced conducted wall heat loads and vessel forces when compared with normal disruptions. One shortcoming of MGI is that the most of the delivered impurities are stopped at the plasma edge and relatively few (typically less than 10%) reach the plasma core on the thermal quench (TQ) timescale [2]. Massive impurity delivery directly to the plasma core is desirable, however, for collisional suppression of runaway electrons (REs) [3]. Wall strikes due to RE beams could compromise vessel integrity and must therefore be avoided in ITER. Investigation of alternate fast shutdown methods to MGI which can deliver impurities to the plasma core effectively is therefore important.

One possible alternate fast shutdown scheme is shell pellet injection. The basic idea is to fire a pellet consisting of a hard shell and dispersive payload at the plasma. The hard shell ablates away as the pellet transits through the plasma edge. On reaching the plasma core, the shell breaks open, releasing the dispersive payload throughout the core region, thus collisionally suppressing RE formation in the tokamak current channel. Two different types of dispersive payloads have been proposed: dust grains [4] or high-pressure gas [5].

In order to design an optimum shell pellet for ITER, the shell material, shell thickness, payload material, and initial pellet velocity must all be carefully considered. The shell should be strong enough to survive being accelerated to high velocity, but thin enough to burn up before reaching the tokamak magnetic axis. Also, the shell material should be as non-perturbative (low-Z) as possible to the tokamak plasma. If the shell is made too high-Z or injected too slowly, the resulting radiative collapse of the current channel could initiate large global magneto-hydrodynamic (MHD) instability, leading to the disruptions TQ before pellet payload delivery has occurred. Also, the pellet needs to be large enough and the payload should disperse well enough through the tokamak current channel to collisionally suppress RE formation. Both shell and payload materials should be chosen to avoid problems with subsequent discharges (i.e. by negatively affecting wall conditioning or pumping systems).

Here, we describe first experiments with shell pellets for disruption mitigation. Small (*o.d.* = 1.8 mm) polystyrene shells were used. Two different designs were tested: cylinders filled with boron powder, and spheres filled with 10 atm argon gas. The pellets were observed to successfully deliver their payloads into the plasma core without significantly perturbing the plasma current channel. The burn-up depth of the pellets is in reasonably good agreement with expectations from ablation rate models.

## 2. EXPERIMENTAL SETUP

The experiments described here were performed on the DIII-D tokamak [6]. Shell pellets were fired into quiescent, H-mode, lower single null deuterium discharges with toroidal magnetic field $B_T = 2.1\,\mathrm{T}$, plasma current $I_p = 1.3\,\mathrm{MA}$, central electron temperature $T_e \approx 2.5\,\mathrm{keV}$, and central electron density $n_e \approx 5\times10^{13}\,\mathrm{cm}^{-3}$. An overview of the pellet trajectory and main diagnostic views is shown in Fig. 1. The pellet is launched from toroidal angle $\phi = 75^{\circ}$ radially inward from the outer midplane. The main diagnostic used to analyze the pellet trajectory is a fast-framing visible camera also located at the outer midplane. Some other crucial diagnostics shown in Fig. 1 are a single-chord, tangentially-viewing UV spectrometer and a 64-chord, radially-viewing fast bolometer system used for fast radiated power measurement at $\phi = 90^{\circ}$.

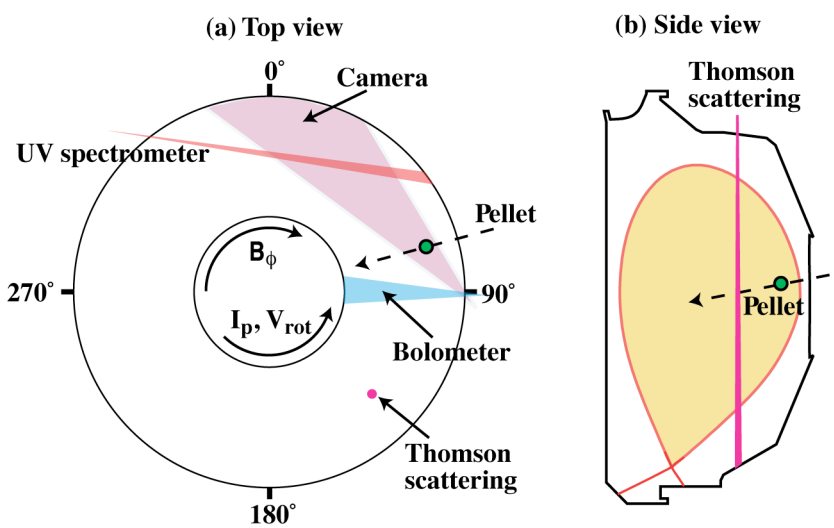


Fig. 1. Overview of pellet trajectory and main diagnostic views.

The pellets are polystyrene ($C_8H_8$) shells, with outer dimensions $D \approx L \approx 1.8$ mm, either cylinders or spheres, both with wall thickness $t \approx 0.37$ mm. Cylinders were machined, filled with boron powder, and then had a sealing cap glued on. The spherical shells were formed and hardened in solution and diffusion evacuated and filled with 10 atm argon.

The pellets are accelerated to about 500 m/s in a pellet launcher using a short pulse of high pressure (500 psi) helium. The pellets are directed into a long ($L \approx 5$ m) curved guide tube for delivery to the tokamak. The pellets were found to slow in the guide tube to about 350 m/s before hitting the plasma. Also, about 1/2 the pellets were found to break before reaching the plasma, presumably due to the bends in the guide tube. The following discussion will focus on results from the pellets which reached the plasma unbroken.

# 3. SHELL BURN-UP

In this section, data from polystyrene spheres is shown. These have a relatively small ($\approx 1.7\times10^{16}$ atoms) argon payload which has only a very small effect on the plasma, simplifying interpretation of the data (i.e. radiated power, density rise, etc. comes from shell, not payload). An overview of a spherical shell pellet experiment is shown in Fig. 2. Pellets are fired into the plasma at times $t$ = 2, 2.25, and 2.5 s. Flashes of radiated power are seen [slow bolometer data from $\phi = 75^{\circ}$ is shown in Fig. 2(a)] and the plasma diamagnetic (thermal) energy $W_{th}$ is observed to drop by about 0.15 MJ, Fig. 2(b). Only a very small drop in plasma current (<4%) is seen, Fig. 2(c), suggesting a very small contraction of the plasma current profile.

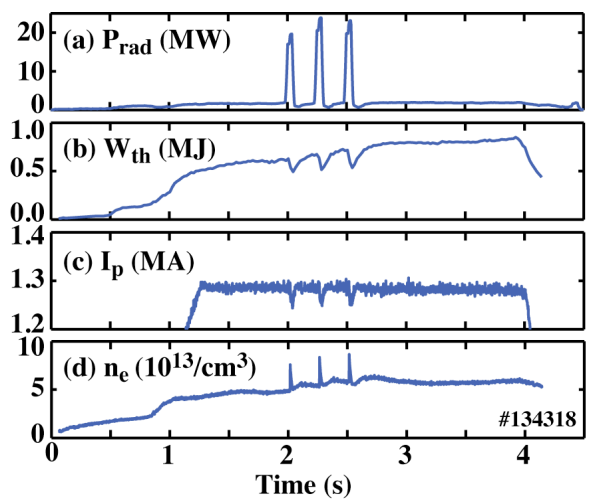


Fig. 2. Overview of shell pellet experiment showing time traces of (a) radiated power $P_{rad}$, (b) plasma thermal energy $W_{th}$, (c) plasma current $I_p$, and (d) line-averaged density $n_e$.

The observed plasma thermal energy drop of 0.15 MJ is consistent with the expected ionization cost of the pellet shell. The spherical pellets consist of 2.49 mg of polystyrene shell and 0.015 mg of argon payload. Ignoring the argon and hydrogen, we have about $2.1\times10^{20}$ atoms of carbon injected, giving an ionization cost of $E_{i,C} \approx 5$ keV per carbon atom. The exact time history of electron temperature seen by carbon in the ablation plume has not been simulated, but single particle simulations of the ionization cost for carbon over the burn-up timescale using CRETIN [7] give results ranging from $E_{i,C} \approx 2.2$ keV at $T_e = 1$ keV and $E_{i,C} \approx 6.6$ keV at $T_e = 200$ eV, roughly consistent with the measured $E_{i,C} \approx 5$ keV.

The pellet motion through the plasma is observed with a fast-framing camera. A false-color image of the pellet ablation plume at three time steps is shown in Fig. 3. From the known camera position and orientation, the pellet location in space can be determined in two

dimensions, as shown in Fig. 4(a). The depth of the pellet along the view chord is constrained by assuming the pellet is traveling on its vacuum trajectory; deviations from this straight line are reflected as error bars in Fig. 4(a); it can be seen that the pellet follows the vacuum trajectory fairly well. The pellet velocity, Fig. 4(b), can be seen to drop significantly in the plasma, from an initial 350 m/s at the plasma edge down to 100 m/s before burning up at normalized radius $\rho = r/a \approx 0.4$.

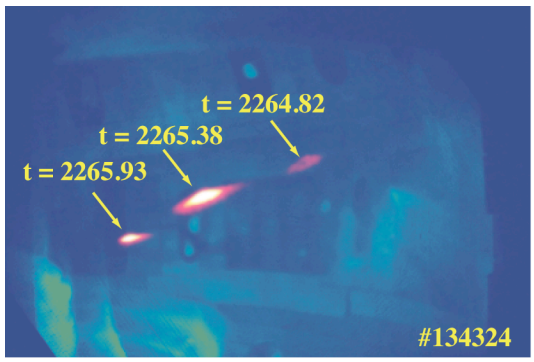


Fig. 3. False-color images ($C_{II}$ emission) of spherical pellet ablation plumes at three time steps.

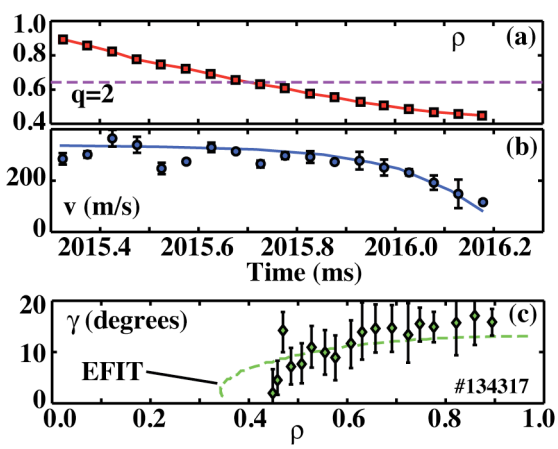


Fig. 4. Time sequence of pellet normalized radius ρ (a) and velocity $v$ (b) calculated from camera images; and observed ablation plume pitch angle compared with EFIT reconstructions of magnetic field pitch angle γ.

The pitch angle of the ablation plume seen in the camera images is expected to follow magnetic field lines to first approximation. This does appear to be the case, as is seen by comparing the measured plume pitch angle with the Grad-Shafranov reconstruction (EFIT) of magnetic pitch angle $\gamma$ along the pellet trajectory, Fig. 4(c).

The pellet shell burning up at $\rho \approx 0.4$ is consistent with Thomson scattering profiles taken immediately before and after the pellet burn-up, shown in Figs. 5(b) and 5(c). It can be seen that the perturbations in $T_e$ and $n_e$ reach in radially to about $\rho \approx 0.4$ or so. Motional Stark effect data, Fig. 5(d), shows that the pellet has had very little effect on the current profile, as seen in the negligible change in the magnetic pitch angle $\gamma$ measured along a neutral beam path. Analysis of wall magnetic loop data indicates that the pellets destabilize only fairly small (~5 G), fairly edge-localized (m/n = q ~ 3) MHD activity, not the large core (2/1) and (1/1) modes associated with the major disruption TQ; this is consistent with the negligible current channel perturbation seen in Fig. 5(d).

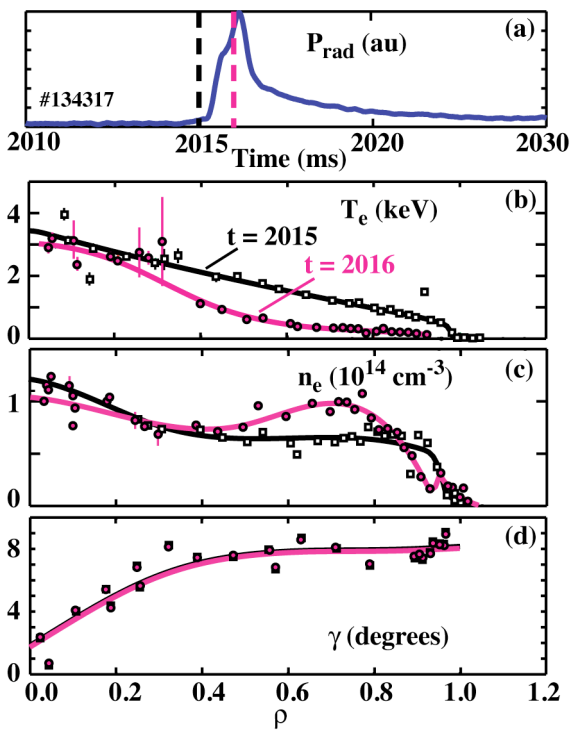


Fig. 5. (a) Time trace of radiated power $P_{rad}$ from fast bolometer showing initial (impact) and final (burn-up) pellet times; initial and final Thomson scattering profiles of (b) $T_e$ and (c) $n_e$; initial and final midplane magnetic pitch angle $\gamma$ along a neutral beam path from motional Stark effect.

Shell pellet burn-up at $\rho \approx 0.4$ is also consistent with fast bolometry, where tomographic reconstruction of line-integrated AXUV photodiode data is used to obtain profiles of total plasma emissivity as a function of time, Fig. 6.

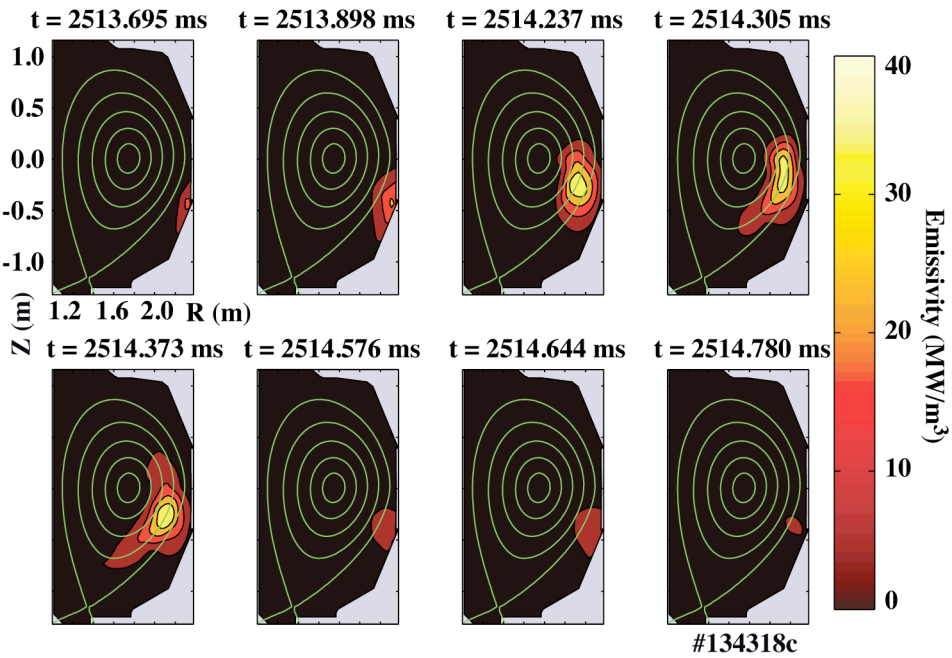


Fig. 6. Fast bolometry showing pellet impurity deposition in to about $\rho \approx 0.4$

# 4. PAYLOAD DISPERSION

Delivery of the pellet payload to the core can be seen in the UV spectrometer data. Figure 7(a) shows single (core tangential) view time traces of line brightnesses of $C_{VI}(18.2\text{ nm})$ and $Ar_{XV}(22.1\text{ nm})$ for a spherical pellet shot. Despite the coarse time resolution (1 ms) of the data, a delay between the shell material (carbon) and payload material (argon) is clear in the data. Similarly, Fig. 7(b) shows data for a cylindrical pellet; a clear delay in the appearance of the payload material (boron in this case) is apparent.

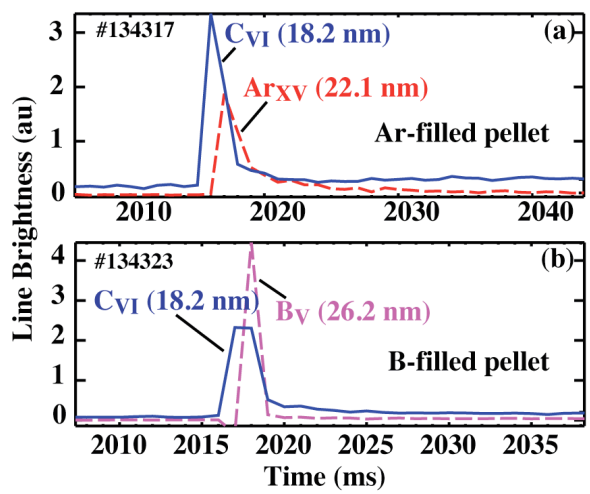


Fig. 7. Time traces of UV line brightnesses from (a) Ar-filled sphere and (b) B-filled cylinder.

The filtered camera images indicate that the deposition of the payload material is quite local. An example of this is shown below: Fig. 8(a) shows time sequences of the total ablation plume brightness of a cylindrical pellet burn-up measured in $B_{II}(412\text{ nm})$ or $C_{II}(514\text{ nm})$. Because the plasma in the vicinity of the pellet is quite dense and because the interference filters used in the visible camera are fairly broad spectrally (FWHM = 5 nm), the measured brightness is a combination of the desired line emission plus broadband emission (bremsstrahlung). Nevertheless, a clear spike in $B_{II}$ emission (relative to $C_{II}$) can be seen in the Fig. 8(a); this is attributed to the release of boron powder from the pellet. The released boron powder does not appear to disperse far from the pellet; this is seen in Fig. 8(b) where the characteristic radius of the $B_{II}$ spot is plotted as a function of time. It can be seen that there is no discernable expansion of the boron cloud, indicating that the boron (at least low charge states) burns up locally in the hot core plasma.

Although payload neutral deposition is quite local, mixing of higher charge state payload ions through the core appears to proceed rapidly. This can be seen in charge-exchange recombination (CER) data. Figure 9(a) shows a time trace of CER line brightness at radius $\rho = 0.57$. The line used, 494 nm, contains a combination of both $C^{5+}$ and $B^{5+}$ contributions. In

the case of a broken pellet (no boron payload), only $C^{5+}$ is present, which ionizes away quickly. In the case of an unbroken pellet with boron payload, the signal at late times (>15 ms after impact) is much larger due to the presence of $B^{5+}$. A simple estimate of $B^{5+}$ profiles can be made by subtracting the two curves at each radius, Fig. 9(b). It can be seen that, within 15 ms of impact, $B^{5+}$ is fairly well mixed throughout the core region. $B^{5+}$ profiles at earlier times cannot be reconstructed accurately because $C^{5+}$ and ($C^{5+}$ + $B^{5+}$) signals are of similar magnitude. The boron densities of Fig. 9(b) are calculated from the measured line brightnesses using charge-exchange cross sections from ADAS [8].

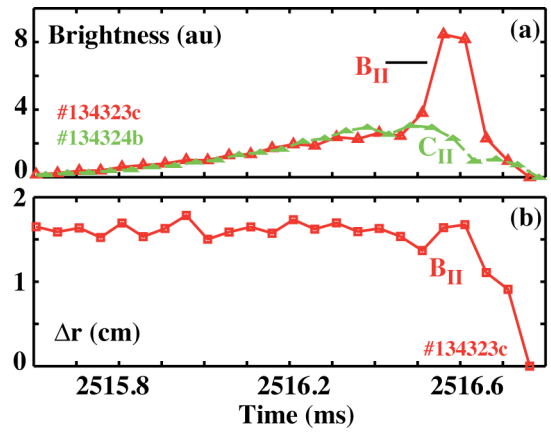


Fig. 8. Time traces of fast camera data of (a) $B_{II}$ and $C_{II}$ brightnesses and (b) $B_{II}$ cloud radius.

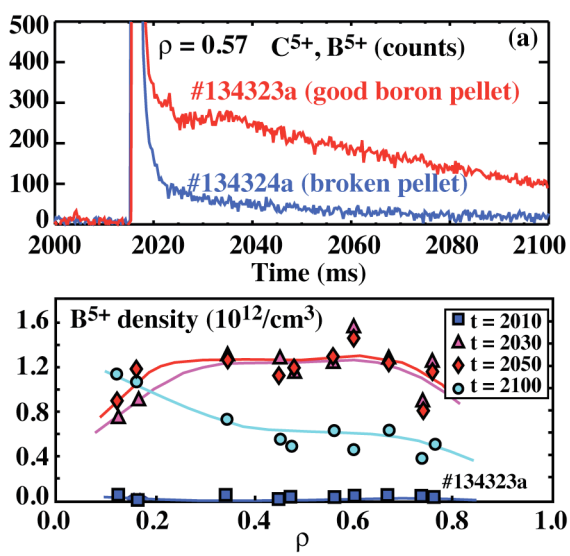


Fig. 9. Charge-exchange recombination spectroscopy at 494 nm showing (a) time traces of whole (boron containing) and broken (empty) cylinder pellets; and (b) calculated radial profiles of $B^{5+}$ density at different time steps.

# 5. SIMULATIONS OF SHELL BURN-UP

The experiments presented here demonstrate successful delivery of compressed gas and dust payloads to the core (current channel) of DIII-D plasmas ahead of any significant current channel contraction. To model the shell burn-up, a simple 1-D (radially varying only; constant on flux surfaces $\psi$) plasma cooling model was constructed. The model uses the measured initial radial profiles of $n_e$ and $T_e$. The injected pellet is assumed to move through the plasma along its vacuum trajectory. The details of the ablation plume moving toroidally away from the pellet are not calculated; instead the cooling of the plasma at each radius is assumed to be limited by the hot electron parallel heat conduction rate to the pellet cross-section, with cross-field heat transport and cross-field particle transport neglected. Total energy loss from each plasma radius is assumed to be limited by the ionization cost of carbon atoms deposited from the pellet shell into that plasma radius, with ionization costs for carbon as a function of plasma temperature calculated using CRETIN. The evolution of the plasma current channel is calculated using a coupled filament model, with ohmic heating neglected. Pellet slowing is assumed to be due to the front/back asymmetry in ablation pressure on the pellet due to the local radial temperature gradient $\nabla T_e$. Ablation rates and pressures are calculated using a neutral gas shielding (NGS) model in the strong ablation shielding limit and including electrostatic shielding (Parks98, Ref. [9]).

Figure 10 shows the simulation results for burn-up of a spherical polystyrene shell with dimensions *o.d.* = 1.8 mm and $t$ = 0.37 mm, and initial velocity $v$ = 350 m/s. It can be seen in Fig. 10(a) (solid line) that the predicted pellet burn-up radius is $\rho \approx 0.55$, which is reasonably close to the measured $\rho \approx 0.45$. The pellet slowing is predicted to drop to only about 340 m/s, inconsistent with the measured 100 m/s. The measured negligibly small current channel perturbation is captured well by the simulation, Fig. 10(d). To compare to a different ablation model, results using the ablation rate for polystyrene suggested by Sergeev [10] is shown by dashed lines in Figs. 10(a) and 10(b). The Sergeev06 ablation model is also a NGS model like Parks98, but does not use electrostatic shielding. Pellet stopping is seen to occur at about $\rho \approx 0.6$, i.e. slightly farther from the measured $\rho \approx 0.45$ than the Parks98 model.

The experiments presented above inject fairly small, weakly-perturbative polystyrene shell pellets. The next step in DIII-D is to inject large shell pellets which inject enough payload material (electrons) to achieve collisional RE suppression. Assuming a typical current quench parallel electric field $E_\varphi \approx 50$ V/m, the required electron density is $n_{crit} \approx 4 \times 10^{16}\,\mathrm{cm}^{-3}$, which, assuming a core volume of 10 $\mathrm{m}^3$, corresponds to an electron number of $N_e \approx 4 \times 10^{23}$. This can be achieved with a thin-walled $D$ = 1 cm shell pellet filled with boron powder, which contains $N_B \approx 1 \times 10^{23}$ boron atoms or $N_e \approx 5 \times 10^{23}$ electrons. Assuming a $L$ = 50 cm launch tube with 500 psi helium drive pressure, an initial pellet velocity of $v \approx 180$ m/s is expected [11]. Figure 11 shows the predicted ablation for a *o.d.* = 1 cm, $t$ = 0.4 mm, initial $v$ = 180 m/s polystyrene sphere fired into DIII-D. A core mass of

1.1 g is assumed (this affects the pellet slowing; the model does not include any effects of pellet payload other than mass). It can be seen in Fig. 11(a) that the pellet reaches well into the core ($\rho \approx 0.2$) before burning up. Because of the larger shell surface area, however, significant temperature and current profile perturbations are expected from the shell alone, Fig. 11(c) and 11(d). It is therefore possible that this large shell will initiate the disruption TQ before reaching $\rho \approx 0.2$ and dispersing its payload material.

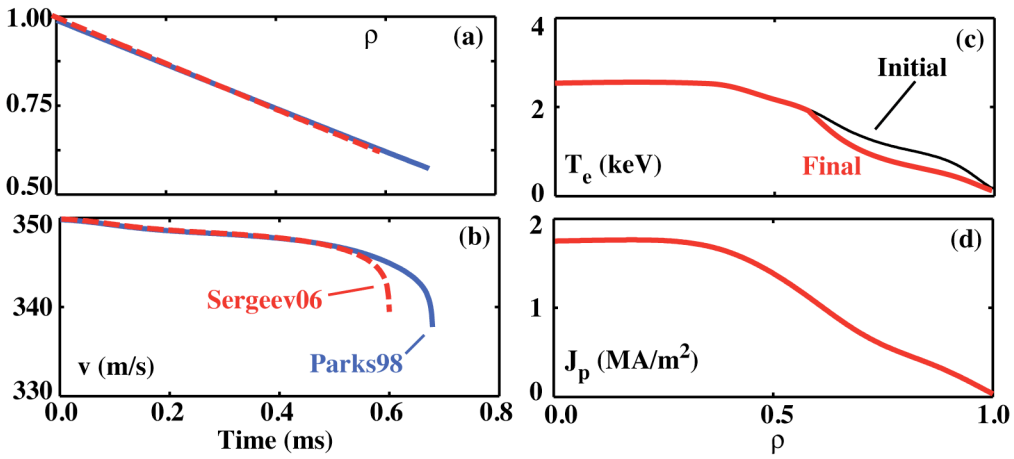


Fig. 10. Simulation of *o.d.* = 1.8 mm, *t* = 0.37 mm spherical polystyrene shell showing time traces of (a) pellet normalized radius ρ and (b) pellet velocity $v$; as well as initial and final radial profiles of (c) electron temperature $T_e$ and (d) plasma current density $J_p$. Solid lines correspond to Parks98 ablation model, dashed lines in (a),(b) use Sergeev06 ablation model.

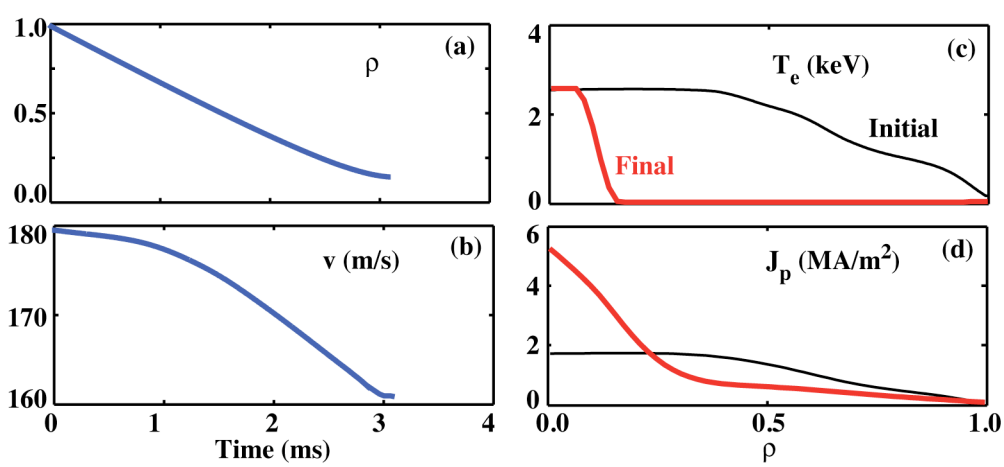


Fig. 11. Simulation of *o.d.* = 1 cm, *t* = 0.4 mm spherical polystyrene shell showing time traces of (a) pellet normalized radius ρ and (b) pellet velocity $v$; as well as initial and final radial profiles of (c) electron temperature $T_e$ and (d) plasma current density $J_p$.

# 6. SUMMARY

Injection of small (*o.d.* = 1.8 mm, $t$ = 0.37 mm) polystyrene shell pellets into DIII-D has provided a proof-of-principle demonstration of pellet payload delivery into the tokamak core (current channel). Measured shell penetration to $\rho \approx 0.45$ before burn-up is roughly matched by ablation rate calculations which give penetration to $\rho \approx 0.55$. Observed pellet slowing from $v$ = 350 m/s down to 100 m/s before burn-up is underestimated by present estimates of slowing based on the radial temperature gradient. The small polystyrene shells do not disrupt the plasma: at the time of shell burn-up, negligible change in current profile has occurred and only very small edge (3/1) MHD is destabilized, unlike the large (2/1), (1/1) modes which lead to the disruption TQ. Deposited payload material is observed to ionize quite locally (within 1 cm of the pellet) and mix as ions rapidly (within 15 ms) through the plasma core.

Future experiments in DIII-D will attempt to inject sufficiently large (*o.d.* = 1 cm) shell pellets to cause collisional suppression of RE. These shells will strongly perturb the plasma, and simulations indicate that significant contraction of the current channel will occur, possibly intiating the TQ. Further experiments and improved modeling are therefore necessary to design a shell pellet which can optimally deliver and disperse sufficient payload material in the current channel ahead of the disruption TQ.

# REFERENCES

[1] T. C. Hender, J. C. Wesley, J. Bialek, et al., *Nucl. Fusion* **47**, S128-S202 (2007).

[2] E. M. Hollmann, T. C. Jernigan, P. B. Parks, et al., *Nucl. Fusion* **48**, 115007 (12pp) (2008).

[3] M. N. Rosenbluth and S. V. Putvinski *Nucl. Fusion* **37**, 1355-1362 (1997).

[4] P. B. Parks, "Dust ball pellets for disruption mitigation," Invention Disclosure DOE Case No. S-113-472 (2007).

[5] T. E. Evans, private communication (2006).

[6] J. L. Luxon, *Nucl. Fusion* **42**, 614 (2002).

[7] H. A. Scott, *J. Quant. Spectrosc. Radiat. Transfer* **71**, 689 (2001).

[8] H. P. Sommers, "Atomic data and analysis structure: user's manual", (JET Joint Undertaking Report JET-IR94, 1994); http://www.adas.ac.uk/.

[9] P. B. Parks and M. N. Rosenbluth, *Phys. Plasmas* **5**, 1380-1386 (1998).

[10] V. Yu. Sergeev, O. A. Bakhareva, B. V. Kuteev, and M. Tendler, *Plasma Phys. Reports* **32**, 363-377 (2006).

[11] L. Baylor, private communication (2009).

## ACKNOWLEDGMENT

This work was supported by the US Department of Energy under DE-FG02-07ER54917, DE-FC02-ER54698, and DE-AC05-00OR22725. The technical support of D. Sundstrom and C. Murphy is gratefully acknowledged, as is the assistance of the DIII-D operations team. The assistance of J.F. Hund, N.B. Alexander, and the rest of the GA IFT group in producing the polystyrene spheres is gratefully acknowledged. Permission from H.A. Scott to use the CRETIN code is gratefully acknowledged. The originating developer of ADAS is the JET Joint Undertaking.